Available online at www.sciencedirect.com
ScienceDirect
Trans. Nonferrous Met. Soc. China 23(2013) 832−840
Transactions of Nonferrous Metals Society of China
www.tnmsc.cn

Predominance diagrams for Zn(II)−NH_3−Cl^-−H_2O system

Zhi-ying DING, Qi-yuan CHEN, Zhou-lan YIN, Kui LIU

Key Laboratory of Resources Chemistry of Nonferrous Metals, School of Chemistry and Chemical Engineering, Central South University, Changsha 410083, China

Received 13 August 2012; accepted 20 November 2012

Abstract: The thermodynamics in zinc hydrometallurgical process was studied using a chemical equilibrium modeling code (GEMS) to predict the zinc solubility and construct the species distribution and predominance diagrams for the Zn(II)−NH_3−H_2O and Zn(II)−NH_3−Cl^-−H_2O system. The zinc solubilities in ammoniacal solutions were also measured with equilibrium experiments, which agree well with the predicted values. The distribution and predominance diagrams show that ammine and hydroxyl ammine complexes are the main aqueous Zn species, $Zn(NH_3)_4^{2+}$ is predominant in weak alkaline solution for both Zn(II)−NH_3−H_2O and Zn(II)−NH_3−Cl^-−H_2O systems. In Zn(II)−NH_3−Cl^-−H_2O system, the ternary complexes containing ammonia and chloride increase the zinc solubility in neutral solution. There are three zinc compounds, $Zn(OH)_2$, $Zn(OH)_{1.6}Cl_{0.4}$ and $Zn(NH_3)_2Cl_2$, on which the zinc solubility depends, according to the total ammonia, chloride and zinc concentration. These thermodynamic diagrams show the effects of ammonia, chloride and zinc concentration on the zinc solubility, which can provide thermodynamic references for the zinc hydrometallurgy.

Key words: thermodynamics; predominance diagram; zinc hydrometallurgy; ammonia leaching

1 Introduction

The combination of ammonia and ammonium salts has been known to be an attractive lixiviant used in hydrometallurgical process for many years due to its low cost and easy regeneration. The major wasteful components, such as Fe, Ca, Mg, Si in ores, are insoluble in ammoniacal solutions. This allows selective extraction of the desired metals and leaving the undesirable components intact with the residue.

The first account of the zinc extractions by ammoniacal solution was published in 1880 as "the Schnabel Process" [1]. This represented the first large-scale use of ammoniacal lixiviant for hydrometallurgy. It thus established the foundation for ammoniacal leaching in copper and nickel hydrometallurgy. Many researches on the leaching of oxidized zinc ores have been carried out in ammoniacal solutions such as $(NH_4)_2CO_3$, $(NH_4)_2SO_4$ or NH_4Cl [2,3]. The process chosen usually depends upon both the composition and the localization of zinc ores. To the knowledge of present authors, two hydrometallurgical processes based on ammonium chloride (NH_4Cl) have successfully been applied in the CENIM-LNETI process for base metals [4] and the Ezinex process for zinc recovery [5]. The use of NH_4Cl shows certain advantages over other ammonium salts. For example, chloride is an aggressive ion which improves the kinetics of dissolution of oxides [6] and sulphides [7]; non-ferrous metals tend to coordinate with chloride ion to dissolve highly in water. Despite the extensive history of ammoniacal extraction in the recovery of zinc, the thermodynamics has not been well understood.

The predominance diagrams provide useful information for the leaching and extraction processes regarding the thermodynamic stable phases, including soluble complexes and solid phases. The ammoniacal leaching process in zinc hydrometallurgy refers to multiple and multiphase species, and the extraction process is associated with their distribution. Some predominance diagrams in such similar systems have been published in the literatures. For instance, JOHNSON and LEJA [8] constructed φ—pH diagram for the Zn−NH_3−H_2O system; the zinc solubility in Zn−NH_3−H_2O solution has been predicted [9,10]; the

Foundation item: Project (74142000023) supported by Postdoctoral Science Foundation of Central South University, China; Project (2012M521547) supported by China Postdoctoral Science Foundation; Project (721500452) supported by the Fundamental Research Funds for the Central Universities, China

Corresponding author: Qi-yuan CHEN; Tel: +86-731-88877364; E-mail: cqy@csu.edu.cn

DOI: 10.1016/S1003-6326(13)62536-4

distributions of soluble complexes in Zn(II)−NH_3−$(NH_4)_2SO_4$−H_2O and Zn(II)−NH_3−$(NH_4)_2CO_3$−H_2O systems have also been investigated [11,12], in which only the simple ions and binary complexes are considered and the range of pH is limited. However, ternary complexes and solids are also formed in real systems. These species are interrelated and play important roles in the leaching and extraction processes in zinc hydrometallurgy. To understand the thermodynamic variation rules in these processes, the predominance diagrams in whole pH range will be constructed to provide more reasonable basic data for zinc hydrometallurgy.

2 Experimental

The solubility measurements in Zn(II)−NH_3−H_2O and Zn(II)−NH_3−Cl^-−H_2O systems were performed by the equilibrium experiments in a closed system to avoid ammonia losses. The reagents included ammonia (25%), ammonium chloride and ZnO (AR grade). All the experiments were carried out at (25±0.1) °C. Solutions were prepared by mixing ammonia/ammonium chloride with distilled water. Then, the solution and excessive amount of ZnO were added in a round-bottomed flask and sealed immediately. The equilibrium time was 15 d, which has been determined from initial experiments. The concentration of zinc was analyzed by ICP-AES method (IRIS Intrepid II XSP, Thermo Fisher Scientific Inc.), and pH value was measured by potentiometric titration.

3 Thermodynamic study

3.1 Thermodynamic model

The thermodynamic diagrams were constructed based on free energy minimization algorithms and simultaneous equilibrium principle, which were used by the chemical equilibrium software GEM-Selektor(GEMS) [13]. The GEMS is a broad-purpose geochemical modeling code, which uses an advanced convex programming method of Gibbs energy minimization implemented in an efficient interior points method numerical module. It can be used to compute equilibrium phase assemblage and speciation in a complex chemical system from its total bulk elemental composition. Chemical interactions involving solids, solid solutions, gas mixtures and aqueous electrolytes are considered simultaneously with elemental stoichiometry. Activity coefficients (γ_i) of aqueous species were computed with the built-in extended Debye-Hückel equation:

$$\lg\gamma_i = \frac{-A_\gamma z_i^2\sqrt{I}}{1+\dot{a}B_\gamma\sqrt{I}} + b_\gamma I \quad (1)$$

where b_γ is a semi-empirical coefficient; $\dot{a}$ is an average distance of approach of two ions of opposite charge; z_i is the charge of species i; I is the effective mole ionic strength; A_γ and B_γ are P and T-dependent coefficients. Equation (1) is applicable up to 1−2 mole ionic strength using b_γ=0.064 and $\dot{a}=10^{-8}$ cm for all ionic species at 25 °C [14]. However, the value of ionic strength in zinc hydrometallurgical process is always greater than 2 mol/kg. Therefore, extrapolation and calibration with experimental data have been performed to reduce the errors in the calculations.

3.2 Thermodynamic data

The GEMS includes a built-in write protected Nagra/PSI chemical thermodynamic database 01/01[15], and a complementary database consisted of Slope98.DAT data [16]. Some equilibrium constants for complex formation were complemented into the thermodynamic database. Then the necessary data were automatically selected for the calculation. The species reported in Refs. [17−20] and the formation constants are shown in Table 1. The data were complemented with the modeling to calculate the equilibrium of Zn(II) in ammoniacal systems.

4 Results and discussion

4.1 Solubility and species distribution for Zn(II)−NH_3−H_2O system

Figure 1 shows the zinc solubility and pH as a function of total ammonia concentration ($[NH_3]_T$) in the Zn(II)−NH_3−H_2O system, in which the experimental results agree very well with the calculated values. Thus it verifies the accuracy of thermodynamic data of relative species. Low zinc solubilities in ammonia solutions are observed even in the solution with $[NH_3]_T$ of 3 mol/kg due to their high pH.

The distribution diagrams of Zn species for the Zn(II)−NH_3−H_2O system are shown in Fig. 2. These diagrams show the mole fraction of Zn species present as a function of pH. No zinc ammine complexes are observed at pH value below 4. As pH increases, $Zn(NH_3)^{2+}$, $Zn(NH_3)_2^{2+}$ and $Zn(NH_3)_3^{2+}$ appear in sequence. $Zn(NH_3)_4^{2+}$ becomes the predominant species at pH 7.0−11.8 (Fig. 2(c)). For a pH range of 11.8−12.5, $Zn(NH_3)_3(OH)^+$ is the predominant complex [17,18]. The mole fraction of solid phase $Zn(OH)_{2(s)}$ was determined to get a maximum at pH 13.2.

In Fig. 2, the increase of $[NH_3]_T$ is helpful for the decrease of $Zn(OH)_{2(s)}$ and the formation of zinc ammine complexes. $Zn(NH_3)_4^{2+}$ produces the highest zinc solubility for one individual species since its mole fraction is around 95% at pH 8.5−10.5, and this is the

Table 1 Zinc complexes and their formation constants (lg$K$) (25 °C, 10^5 Pa)

Species type	Species	Equation	lg$K$	Reference
Hydrolysis products	$Zn(OH)^+$	$Zn^{2+}+H_2O=Zn(OH)^++H^+$	−7.5	[21]
	$Zn(OH)_{2(aq)}$	$Zn^{2+}+2H_2O=Zn(OH)_{2(aq)}+2H^+$	−16.4	[21]
	$Zn(OH)_{2(s)}$	$Zn^{2+}+2H_2O=Zn(OH)_{2(s)}+2H^+$	−12.4	[22]
	$Zn(OH)_3^-$	$Zn^{2+}+3H_2O=Zn(OH)_3^-+3H^+$	−28.2	[21]
	$Zn(OH)_4^{2-}$	$Zn^{2+}+4H_2O=Zn(OH)_4^{2-}+4H^+$	−41.2	[22]
	$Zn_2(OH)^{3+}$	$2Zn^{2+}+H_2O=Zn_2(OH)^{3+}+H^+$	−9.0	[22]
	$Zn_2(OH)_6^{2-}$	$2Zn^{2+}+6H_2O=Zn_2(OH)_6^{2-}+6H^+$	−57.8	[22]
Chloride complexes	$ZnCl^+$	$Zn^{2+}+Cl^-=ZnCl^+$	−0.5	[23]
	$ZnCl_{2(aq)}$	$Zn^{2+}+2Cl^-=ZnCl_{2(aq)}$	0.02	[24]
	$ZnCl_3^-$	$Zn^{2+}+3Cl^-= ZnCl_3^-$	0	[23]
	$ZnCl_4^{2-}$	$Zn^{2+}+4Cl^-= ZnCl_4^{2-}$	0.10	[23]
Ammine complexes	$Zn(NH_3)^{2+}$	$Zn^{2+}+NH_3=Zn(NH_3)^{2+}$	2.35	[22]
	$Zn(NH_3)_2^{2+}$	$Zn^{2+}+2NH_3= Zn(NH_3)_2^{2+}$	4.80	[22]
	$Zn(NH_3)_3^{2+}$	$Zn^{2+}+3NH_3= Zn(NH_3)_3^{2+}$	7.31	[22,25]
	$Zn(NH_3)_4^{2+}$	$Zn^{2+}+4NH_3= Zn(NH_3)_4^{2+}$	9.46	[22,25]
Monohydroxy ammine complexes	$Zn(NH_3)(OH)^+$	$Zn^{2+}+NH_3+OH^-= Zn(NH_3)(OH)^+$	9.23	[18]
	$Zn(NH_3)_2(OH)^+$	$Zn^{2+}+2NH_3+OH^-= Zn(NH_3)_2(OH)^+$	10.80	[17,18]
	$Zn(NH_3)_3(OH)^+$	$Zn^{2+}+3NH_3+OH^-= Zn(NH_3)_3(OH)^+$	12.00	[17,18]
Dihydroxy ammine complexes	$Zn(NH_3)(OH)_{2\,(aq)}$	$Zn^{2+}+NH_3+2OH^-= Zn(NH_3)(OH)_{2\,(aq)}$	13.00	[17]
	$Zn(NH_3)_2(OH)_{2(aq)}$	$Zn^{2+}+2NH_3+2OH^-= Zn(NH_3)_2(OH)_{2(aq)}$	13.60	[17,18]
Trihydroxy ammine complexes	$Zn(NH_3)(OH)_3^-$	$Zn^{2+}+NH_3+3OH^-= Zn(NH_3)(OH)_3^-$	14.50	[17,18]
Ammonia chloride complexes	$Zn(NH_3)Cl_3^-$	$Zn^{2+}+3Cl^-+NH_3= Zn(NH_3)Cl_3^-$	3.15	[19]
	$Zn(NH_3)_3Cl^+$	$Zn^{2+}+Cl^-+3NH_3= Zn(NH_3)_3Cl^+$	7.90	[20]
	$Zn(NH_3)_2Cl_{2(s)}$	$Zn^{2+}+2NH_3+2Cl^- = Zn(NH_3)_2Cl_{2(s)}$	7.11	[26]
Oxychloride complexes	$ZnOHCl_{(aq)}$	$Zn^{2+}+Cl^-+OH^-= ZnOHCl_{(aq)}$	6.51	[27]
	$Zn(OH)_{1.6}Cl_{0.4(s)}$	$Zn^{2+}+1.6OH^-+0.4Cl^- = Zn(OH)_{1.6}Cl_{0.4(s)}$	14.2	[20,24]

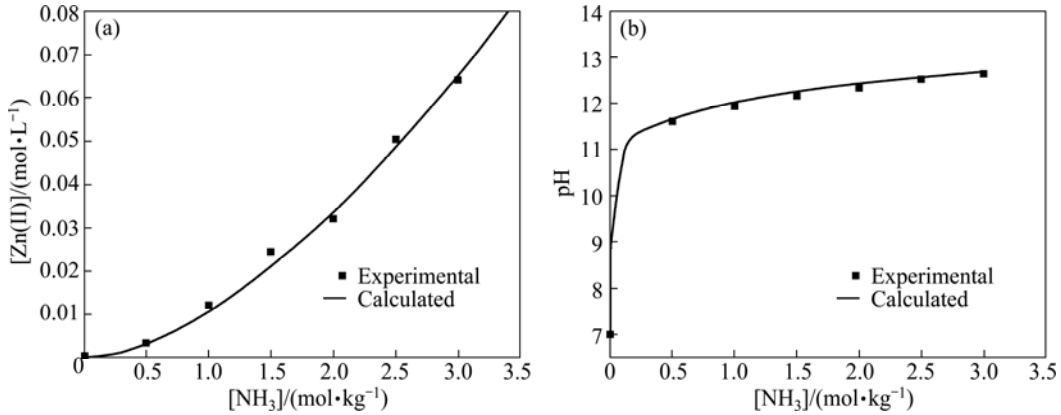

Fig. 1 Zinc solubility (a) and pH (b) in Zn(II)−NH_3−H_2O system

main reason for obtaining high zinc extraction with higher $[NH_3]_T$ in ammoniacal leaching process.

4.2 Solubility and species distribution for Zn(II)−NH_3−Cl^-−H_2O system

The experimental and calculated values of zinc solubility and pH in the Zn(II)−NH_3−Cl^-−H_2O system are shown in Fig. 3, which illustrates that the experimental results are consistent with the calculated values. Thus the accuracy of the thermodynamic data of complexes containing chloride is verified. The zinc solubility is greatly increased in the presence of ammonium chloride due to the formation of the buffer solution. The highest zinc solubility is produced in the solution of the ammonia and ammonium chloride mole ratio of 1:1 and the pH is 9.6.

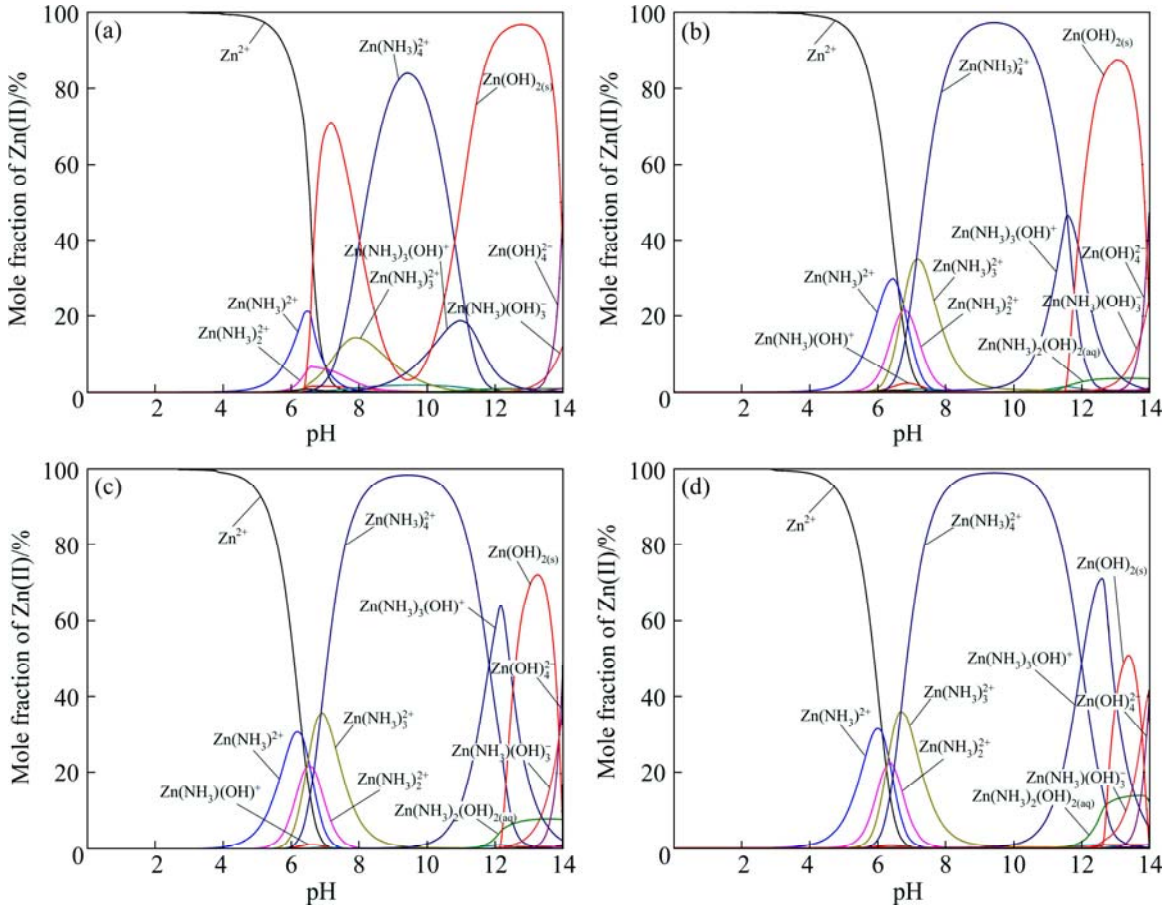

Fig. 2 Zn species distribution diagrams for Zn(II)−NH_3−H_2O system ($[Zn(II)]_T$ 0.2 mol/kg (including Zn(II) in solid and aqueous phases): (a) 1 mol/kg $[NH_3]_T$; (b) 2 mol/kg $[NH_3]_T$; (c) 3 mol/kg $[NH_3]_T$; (d) 4 mol/kg $[NH_3]_T$

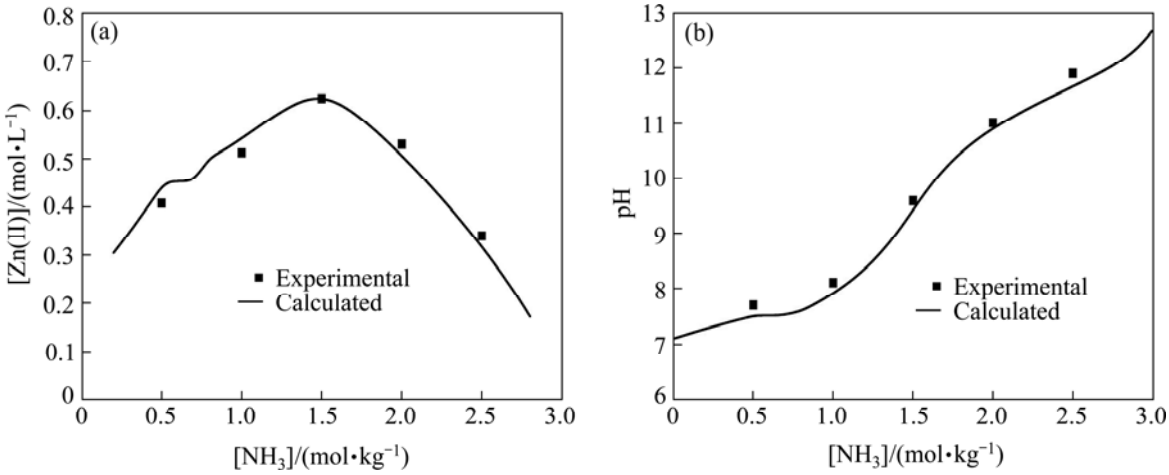

Fig. 3 Zinc solubility (a) and pH (b) in Zn(II)−NH_3−Cl^-−H_2O system

Figure 4 shows the Zn species distribution diagrams for the Zn(II)−NH_3−Cl^-−H_2O system with a concentration of 0.2 mol/kg $[Zn(II)]_T$, 3 mol/kg $[NH_3]_T$ and 1−2.5 mol/kg $[Cl^-]_T$ (total chloride concentration). Giving the predominance of NH_4^+ at pH below 4, free Zn^{2+} and chloride complexes $ZnCl_n^{2-n}$ (n=1, 2, 3, 4) account for most of the total zinc concentration. As the pH increases, ammine and ammonia chloride complexes are present. $Zn(NH_3)_4^{2+}$ becomes the predominant species at pH 7.0−11.8. For pH>10, the Zn species distribution is the same as that in Zn(II)−NH_3−H_2O system. The solid phases evaluated are $Zn(NH_3)_2Cl_{2(s)}$ and $Zn(OH)_{2(s)}$, as reported in Refs. [19,20]. $Zn(NH_3)_2Cl_{2(s)}$ is precipitated in a pH range of 6−7, and $Zn(OH)_{2(s)}$ is present at pH>12.5.

$[Cl^-]_T$ has significant effects on the Zn species

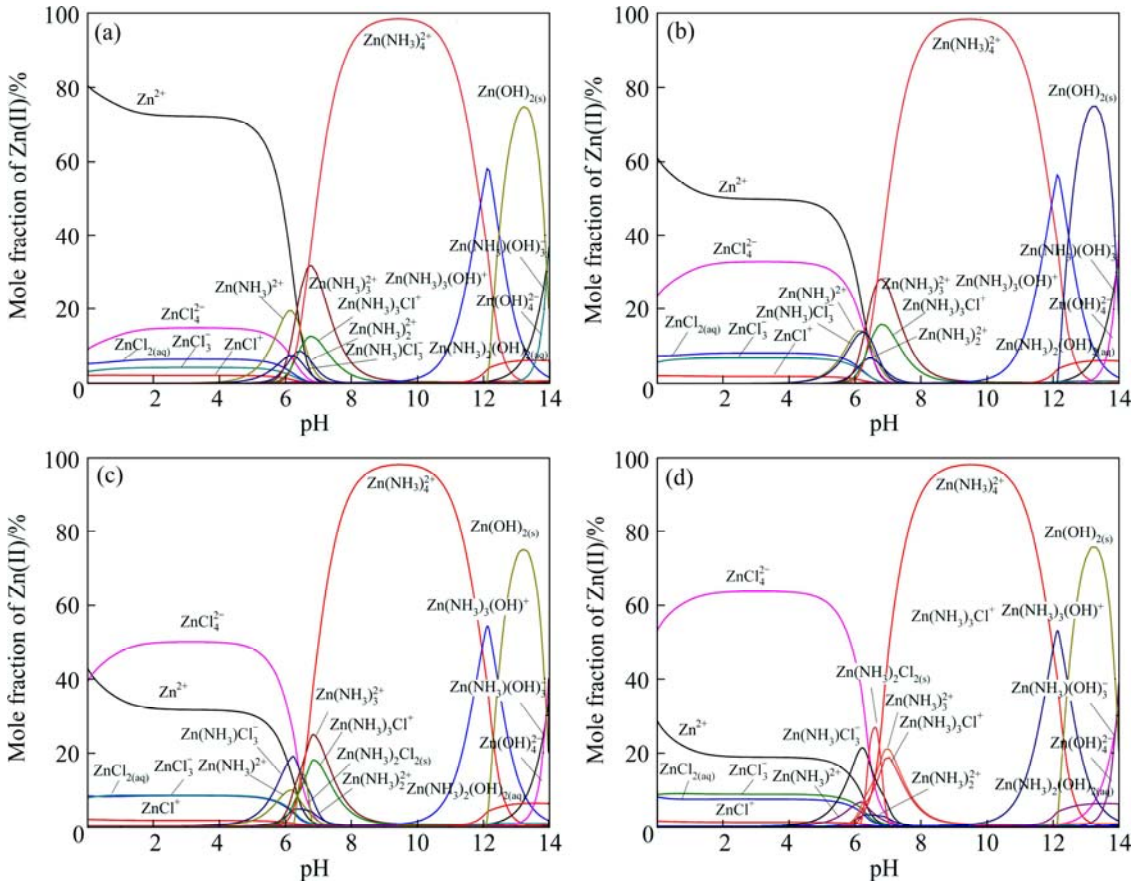

Fig. 4 Zn species distribution diagrams for Zn(II)−NH_3− Cl^-−H_2O system: (a) 1.0 mol/kg $[Cl^-]_T$; (b) 1.5 mol/kg $[Cl^-]_T$; (c) 2.0 mol/kg $[Cl^-]_T$; (d) 2.5 mol/kg $[Cl^-]_T$ ($[Zn(II)]_T$ 0.2 mol/kg; $[NH_3]_T$ 3 mol/kg)

distribution at pH<7. The higher the $[Cl^-]_T$ is, the more the hypercoordinate complexes containing chloride will form. $Zn(NH_3)_2Cl_{2(s)}$ precipitates with higher $[Cl^-]_T$ (Figs. 4(c) and (d)). At pH>9.5 there is no influence of $[Cl^-]_T$ on the Zn species distribution because there is no complex containing chloride.

Figure 5 shows the activity logarithm of free Cl^-, NH_3(aqueous), NH_4^+ and Zn^{2+} as a function of pH for the Zn(II)−NH_3−Cl^-−H_2O system at 25 °C, in which the precipitation conditions of solid phase are also exhibited. According to the reaction equilibrium constant of free NH_3 and NH_4^+, the activity relation between free NH_3 and NH_4^+ can be described as

$$\lg a_{NH_4^+} = \lg a_{NH_3} - pH + 9.24 \quad (2)$$

Thus NH_4^+ is the main ammonia-species at pH<9.24, while pH>9.24, NH_3 is dominant. The activity of Cl^- has little change over the studied pH range. But the activity of Zn^{2+} changes a lot. For 6<pH<7, free Zn^{2+} involves in the coordination to form aqueous complexes and solid phase, which leads to the decrease of Zn^{2+} activity. Then it keeps decreasing due to the formation of $Zn(NH_3)_4^{2+}$. When $Zn(NH_3)_3(OH)^+$ is

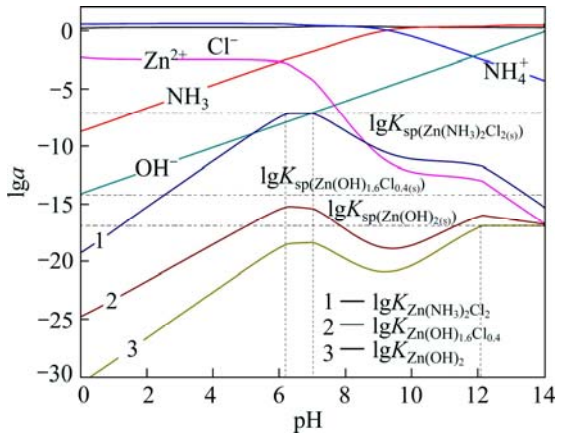

Fig. 5 Activity logarithm diagram of free Cl^-, NH_3, NH_4^+, OH^-, Zn^{2+} and formation of solids for Zn(II)−NH_3−Cl^-−H_2O system (0.2 mol/kg $[Zn(II)]_T$, 3 mol/kg $[NH_3]_T$, 2.5 mol/kg $[Cl^-]_T$)

formed, the decreasing rate of Zn^{2+} activity slows down at pH>10. Until $Zn(OH)_{2(s)}$ separates, the Zn^{2+} activity sharply decreases.

When solids precipitate, the relationships between ionic activities and solubility product constants can be listed as follows:

$$\lg K_{Zn(NH_3)_2Cl_2} = \lg a_{Zn^{2+}} + 2\lg a_{NH_3} + 2a_{Cl^-} \quad (3)$$

$$\lg K_{Zn(OH)_{1.6}Cl_{0.4}} = \lg a_{Zn^{2+}} + 1.6\lg a_{OH^-} + 0.4\lg a_{Cl^-} \quad (4)$$

$$\lg K_{Zn(OH)_2} = \lg a_{Zn^{2+}} + 2\lg a_{OH^-} \quad (5)$$

In Fig. 5, when the value of right side in Eq. (3) reaches the solubility line of $Zn(NH_3)_2Cl_{2(s)}$ at pH 6.2−7.1, $Zn(NH_3)_2Cl_{2(s)}$ precipitates. Similarly, $Zn(OH)_{2(s)}$ precipitates at pH>12.1. But the stoichiometric logarithm sum of ionic activities in Eq. (5) do not reach the solubility line of $Zn(OH)_{1.6}Cl_{0.4(s)}$ in Fig. 5, no $Zn(OH)_{1.6}Cl_{0.4(s)}$ precipitates in the system of 0.2 mol/kg $[Zn(II)]_T$, 3 mol/kg $[NH_3]_T$ and 2.5 mol/kg $[Cl^-]_T$.

4.3 Predominance diagrams for Zn(II)

4.3.1 Construction of predominance diagrams

The predominance diagrams in this study are constructed based on the equilibrium reactions of predominant species. The plotting method is different from the traditional predominance diagrams. Taking the $-\lg[NH_3]_T$—pH diagram of the Zn−NH_3−H_2O system for an example, if $[Zn(II)]_T$ is fixed as 0.2 mol/kg, for every total ammonia concentration, the molality logarithm distribution diagram of Zn species can be calculated as a function of pH(Fig. 6). Thus each pH is corresponding to one species with the maximum concentration in each molality logarithm distribution diagram. Taking $-\lg[NH_3]_T$, pH and molality logarithm of predominant species as *x*-, *y*- and *z*- axis, respectively, a series of surface diagrams similar with Fig. 7 could be figured. The intersecting line between two surfaces is the boundary of two predominant species. To project the boundary line to the *x*−*y* plane, a curve between two predominant species in *x*−*y* plane was obtained. Similarly, boundary curves of another predominant species could be plotted to get a series of closed areas in $-\lg[NH_3]_T$—pH plane. Thus the predominance diagram can be constructed as a function of $[NH_3]_T$ versus pH. Smaller step of $[NH_3]_T$, $[Zn(II)]_T$ and pH will produce more accurate boundary curves. The step of this study is of 0.01.

4.3.2 Predominance diagrams for Zn(II)−NH_3−H_2O system

To determine the formation of soluble and solid phases under different conditions for the Zn(II)−NH_3−H_2O system, independent predominance diagrams were constructed as a function of $[Zn(II)]_T$, $[NH_3]_T$ versus pH. In all diagrams, the dot lines indicate the conditions to be evaluated in this study. Figure 8 shows the predominance diagrams for the Zn(II)−NH_3−H_2O system, which gives some differences from Pourbaix diagrams. Since the boundaries are not derived from the reaction equilibrium of only two adjacent dominant species, but corresponding to the simultaneous equilibrium of all the possible species, some boundaries are curved.

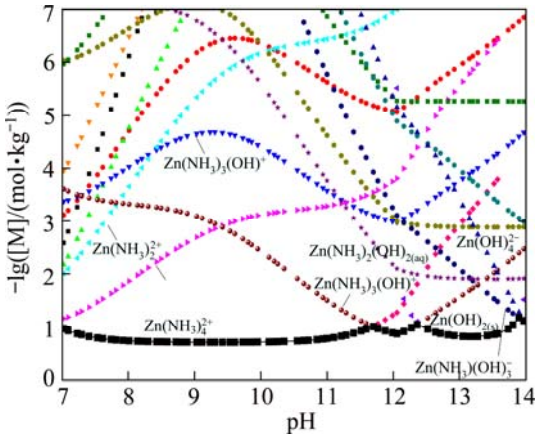

Fig. 6 Molality logarithm distribution diagram of Zn species (M) for Zn(II)−NH_3−H_2O system (0.2 mol/kg $[Zn(II)]_T$, 3 mol/kg $[NH_3]_T$)

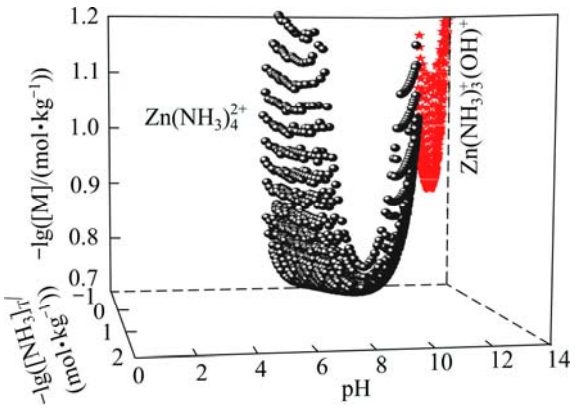

Fig. 7 Surface plot of molality logarithm of predominant species $Zn(NH_3)_4^{2+}$ and $Zn(NH_3)_3(OH)^+$

In Fig. 8(a), curve 1 is the boundary of solid and aqueous species due to the complexing reactions involved. Curve 2 represents the boundary between $Zn(NH_3)_4^{2+}$ and $Zn(NH_3)_3(OH)^+$. Although curve 2 is a straight-line, it is still the results of simultaneous equilibrium, but the effects of other species in regions II and III on the dominant species are negligible. Similarly, curve 3 exhibits linear relation.

In Fig. 8, there is a large predominant zone of Zn^{2+} in acidic region. The predominant zone of $Zn(NH_3)^{2+}$ is narrow as the same as that of $Zn(NH_3)_3^{2+}$ in nearly neutral region. With $[NH_3]_T$>0.64 mol/kg ($-\lg[NH_3]_T$< 0.194), the predominance zone of $Zn(NH_3)_4^{2+}$ appears, which is strongly affected by change in total ammonia concentration. For pH>11.5, $Zn(NH_3)_3(OH)^+$ predominates as far as $[NH_3]_T$ is higher than 1.60 mol/kg, and the pH range of this area is enlarged until $[NH_3]_T$ is around 5.2 mol/kg. When $[NH_3]_T$ is about 2.9 mol/kg, the

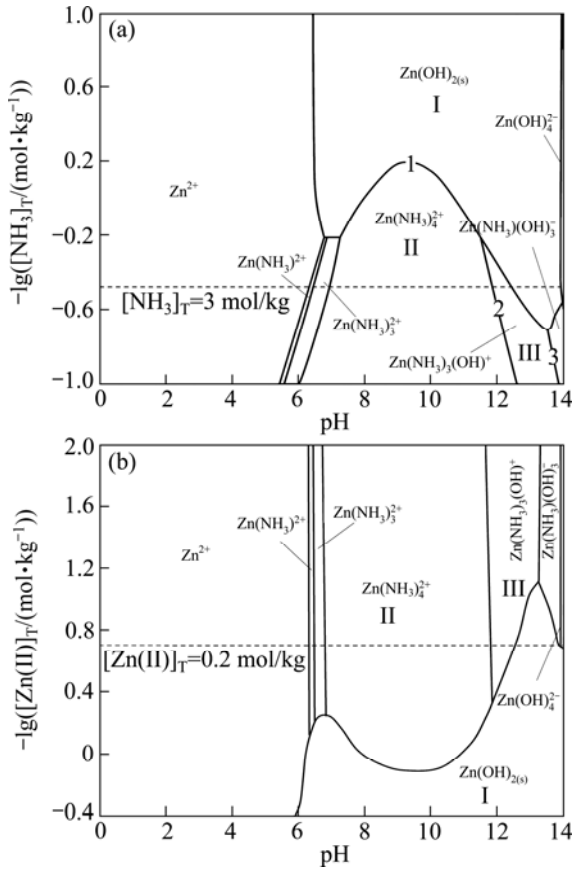

Fig. 8 Predominance diagrams for Zn(II)−NH_3−H_2O system: (a) 0.2 mol/kg $[Zn(II)]_T$; (b) 3 mol/kg $[NH_3]_T$

predominant zones of $Zn(NH_3)(OH)_3^-$ and $Zn(OH)_4^{2-}$ are present with pH>13.64 and pH>13.97, respectively.

4.3.3 Predominance diagram for Zn(II)−NH_3−Cl^-−H_2O system

Figure 9 shows the predominance diagrams for the Zn(II)−NH_3−Cl^-−H_2O system as a function of $[Zn(II)]_T$, $[NH_3]_T$ and $[Cl^-]_T$ versus pH. It can be observed that three solid phases are formed, two in neutral zone, $Zn(NH_3)_2Cl_{2(s)}$ and $Zn(OH)_{1.6}Cl_{0.4(s)}$, and the other in alkaline zone, $Zn(OH)_{2(s)}$. As $[NH_3]_T$ increases, the predominant zone of $Zn(NH_3)_2Cl_{2(s)}$ shifts to the left, then $Zn(NH_3)_2Cl_{2(s)}$ could precipitate in weak acidic zone (Fig. 9(a)). Moreover, the increase of $[Cl^-]_T$ makes it the right slight (Fig. 9(b)). The predominance zone of $Zn(OH)_{1.6}Cl_{0.4(s)}$ appears with $[NH_3]_T$<1.1 mol/kg and 6.8<pH<7.6. For $[NH_3]_T$<1 mol/kg, the predominant zone of $Zn(OH)_{2(s)}$ broadens to neutral region, which is adjacent to $Zn(OH)_{1.6}Cl_{0.4(s)}$. Thus two solid phases can co-exist. Figure 9(c) shows the highest zinc solubility at pH 9.6, which agrees with the experimental results in Fig. 3. The adjacent zones and the intersecting of three solid phases are also present, which illustrates that the co-existence of three solid phases must be present in the Zn(II)−NH_3−Cl^-−H_2O system. LIMPO and LUIS [19] found the co-existence of two solid phases when determining the solubility of $ZnCl_2$ in NH_4Cl solution. For the Zn(II)−NH_3−Cl^-−H_2O system, the phase law is

$$f=C-\Phi+n \quad (6)$$

where f is degree of freedom; C is independent species, C=4; Φ is phase number; n is external factor such as T, P, n=0. Therefore, f=4−Φ, thus the maximum phase number is 4, which indicates that the co-existence of three solid phases agrees with the phase rule.

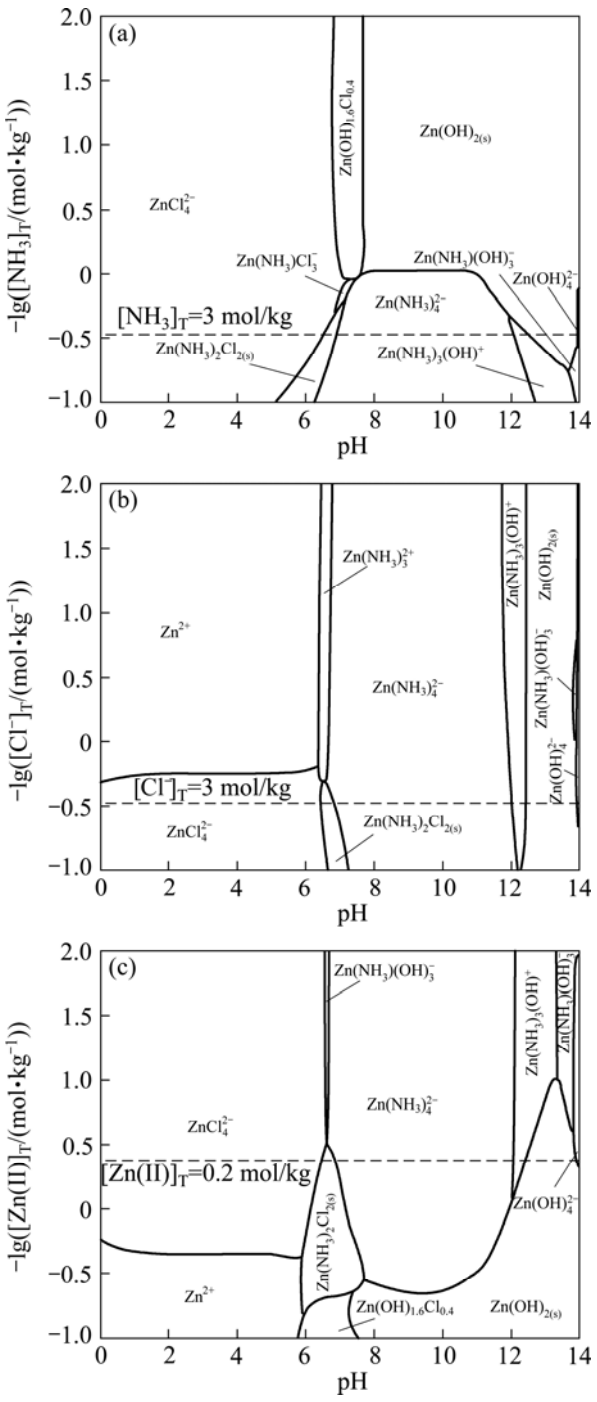

Fig. 9 Predominance diagrams for Zn(II)−NH_3−Cl^-−H_2O system: (a) 0.2 mol/kg $[Zn(II)]_T$, 3 mol/kg $[Cl^-]_T$; (b) 0.2 mol/kg $[Zn(II)]_T$, 3 mol/kg $[NH_3]_T$; (c) 3 mol/kg $[NH_3]_T$ and $[Cl^-]_T$

In acid zone, $ZnCl_4^{2-}$ is the predominant species with $[Cl^-]_T$>1.8 mol/kg, otherwise, Zn^{2+} is the main species (Fig. 9(b)). There is a narrow predominant zone of $Zn(NH_3)_3^{2+}$ with $[Cl^-]_T$<2 mol/kg. $Zn(NH_3)Cl_3^-$ can co-exist with $ZnCl_4^{2-}$, $Zn(NH_3)_4^{2+}$, $Zn(NH_3)_2Cl_{2(s)}$ and $Zn(OH)_{1.6}Cl_{0.4(s)}$. The predominant zone of $Zn(NH_3)_4^{2+}$ is broad for 7.0<pH<11.8. As the pH increases, the predominance zones of $Zn(NH_3)_3(OH)^+$ and $Zn(NH_3)(OH)_3^-$ are also present as the same as those in the Zn(II)−NH_3−H_2O system. The solubility of $Zn(OH)_{2(s)}$ reaches a minimum at pH 13.2.

5 Conclusions

1) The zinc solubilities in the Zn(II)−NH_3−H_2O and Zn(II)−NH_3−Cl^-−H_2O systems were determined with equilibrium experiments, which agree well with the predicted values. The Zn species distribution and predominance diagrams for the Zn(II)−NH_3−H_2O and Zn(II)−NH_3−Cl^-−H_2O systems were constructed using a chemical equilibrium software.

2) For the Zn(II)−NH_3−H_2O system, ammine and hydroxyl ammine complexes are the main aqueous species in neutral and alkaline zones. $Zn(NH_3)_4^{2+}$ is predominant species in weak alkaline zone. There is one solid phase, $Zn(OH)_{2(s)}$, which determines the zinc solubility.

3) In alkaline zone of the Zn(II)−NH_3−Cl^-−H_2O system, species distribution and predominance diagrams are the same as those of Zn(II)−NH_3−H_2O system. In neutral zone, the ternary complexes containing ammonia and chloride appear. There are three solid phases, $Zn(OH)_{1.6}Cl_{0.4}$, $Zn(NH_3)_2Cl_2$ and $Zn(OH)_2$. The zinc solubility is determined by the one of the three solid phases, depending on the concentration of total zinc, ammonia and chloride. For the higher $[NH_3]_T$ and $[Cl^-]_T$, the lower $[Zn(II)]_T$, it is the $Zn(NH_3)_2Cl_2$; while for the lower $[NH_3]_T$, the higher $[Cl]_T$ and $[Zn(II)]_T$, it is $Zn(OH)_{1.6}Cl_{0.4}$; and for the very lower $[NH_3]_T$ and $[Cl]_T$, the higher $[Zn(II)]_T$, it is $Zn(OH)_2$. Zinc solubility increases quickly when total ammonia and chloride concentrations increase in weak alkaline solution. Thus the predominance diagrams are helpful for the controlling in zinc hydrometallurgical process.

References

[1] HARVEY T G. The hydrometallurgical extraction of zinc by ammonium carbonate: A review of the schnabel process[J]. Mineral Processing and Extractive Metallurgy Review, 2006, 27(4): 231−279.

[2] YOUCAI Z, STANFORTH R. Integrated hydrometallurgical process for production of zinc from electric arc furnace dust in alkaline medium[J]. Journal of Hazardous Materials, 2000, 80(1−3): 223−240.

[3] WANG Rui-xiang, TANG Mo-tang, YANG Sheng-hai, ZHANG Wen-hai, TANG Chao-bo. Leaching kinetics of low grade zinc oxide ore in NH_3−NH_4Cl−H_2O system[J]. Journal of Central South University of Technology, 2008, 15(5): 679−683.

[4] LIMPO J L, FIGUEIREDO J M, AMER S, LUIS A. The CENIM-LNETI process: A new process for the hydrometallurgical treatment of complex sulphides in ammonium chloride solutions [J]. Hydrometallurgy, 1992, 28(2): 149−161.

[5] OLPER M. The EZINEX process—A new and advanced way for electrowinning from a chlorine solution [R]. International Symposium—World Zinc '93. Malbourne: The Australasian Institute of Mining and Metallurgy, 1993: 491−494.

[6] EK C, FRENAY J, HERMAN J. Oxidized copper phase precipitation in ammoniacal leaching-the influence of ammonium salt additions [J]. Hydrometallurgy, 1982, 8(1): 17−26.

[7] WINAND R. Chloride hydrometallurgy [J]. Hydrometallurgy, 1991, 27(3): 285−316.

[8] JOHNSON H E, LEJA J. On the potential/pH diagrams of the Cu−NH_3−H_2O and Zn−NH_3−H_2O systems [J]. Journal of the Electrochemical Society, 1965, 112(6): 638−641.

[9] ZHONG Zhu-qian, MEI Guang-gui. Application of diagrams of chemical potential in hydrometallurgy and purification of waste water [M]. Changsha: Central South University of Technology Press, 1986. (in Chinese)

[10] GUBELIET A O, STE-MARIE J. Formation et stabilité de complexes hydroxo-ammonio en solution aqueuse. I. Complexes de zinc [J]. Canadian Journal of Chemistry, 1968, 46(10): 1707−1714.

[11] WANG Rui-xiang, TANG Mo-tang, YANG Jian-guang, YANG Sheng-hai. Thermodynamics of Zn(II) complex equilibrium in system of Zn(II)−NH_3−Cl^-−CO_3^{2-}−H_2O [J]. The Chinese Journal of Nonferrous Metals, 2008, 18(s1): s192−s198. (in Chinese)

[12] TANG Mo-tang, ZHANG Peng, HE Jing, YUAN Xia, CHEN Yong-ming. Leaching zinc dust in system of Zn(II)−$(NH_4)_2SO_4$−H_2O [J]. Journal of Central South University: Science and Technology, 2007, 38(5): 867−872. (in Chinese)

[13] KULIK D A. GEMS-PSI version 2.3.0 rc8 [S]. Villigen, Switzerland. Available from http://gems.web.psi.ch., 2009.

[14] PEARSON F J, BERNER U. Nagra thermochemical data base. 1. Core data [R]. Nagra, Wettingen, 1991.

[15] HUMMEL W, BERNER U, CURTI E, PEARSON F J, THOENEN T. Nagra/PSI chemical thermodynamic database 01/01 [J]. Radiochimica Acta, 2002, 90(9−11): 805−813.

[16] JOHNSON J W, OELKERS E H, HELGESON H C. SUPCRT92—A software package for calculating the standard molal thermodynamic properties of minerals, gases, aqueous species, and reactions from 1 bar to 5000 bar and 0 to 1000 degrees C [J]. Computers & Geosciences, 1992, 18: 899−947.

[17] KRAVTSOV V I, TSVENTARNYI E G, KURTOVA O Y, NOSOV S N. Kinetics and mechanism of electroreduction of ammonia and hydroxyammonia complexes of zinc(II) on a dropping mercury electrode [J]. Russian Journal of Electrochemistry, 2001, 37(6): 559−568.

[18] CRAWFORD R J, MAINWARING D E, HARDING I H. Adsorption and coprecipitation of heavy metals from ammoniacal solutions using hydrous metal oxides [J]. Colloids and Surfaces A: Physicochemical and Engineering Aspects, 1997, 126(2−3): 167−179.

[19] LIMPO J L, LUIS A. Solubility of zinc chloride in ammoniacal ammonium chloride solutions [J]. Hydrometallurgy, 1993, 32(2): 247−260.

[20] LIMPO J L, LUIS A, CRISTINA M C. Hydrolysis of zinc chloride in aqueous ammoniacal ammonium chloride solutions [J]. Hydrometallurgy, 1995, 38(3): 235−243.

[21] ZHANG Y, MUHAMMED M. Critical evaluation of thermodynamics of complex formation of metal ions in aqueous solutions VI. Hydrolysis and hydroxo-complexes of Zn^{2+} at 298.15 K [J]. Hydrometallurgy, 2001, 60(3): 215−236.

[22] IUPAC stability constants database. Sc-database, and mini-scdatabase [M]. Timble, UK: Academic Software, 2001.
[23] MARTELL A E, SMITH R M. Critical stability constants: First supplement [M]. Vol.5. New York: Plenum Press, 1982.
[24] MARTELL A E, SMITH R M. Critical stability constants: Inorganic complexes [M]. Vol.4. New York: Plenum Press, 1976.
[25] SPEIGHT J G. Lange's handbook of chemistry [M]. 16th ed. London: McGraw-Hill, Inc, 2005.
[26] LARCIN J, MASKELL W C, TYE F L. Leclanché cell investigations I: $Zn(NH_3)_2Cl_2$ solubility and the formation of $ZnCl_2·4Zn(OH)_2·H_2O$ [J]. Electrochimica Acta, 1997, 42(17): 2649−2658.
[27] WAGMAN D D, EVANS W H, PARKER V B. The NBS tables of chemical and thermodynamic properties: Selected values for inorganic and C1 and C2 organic substances in si units [J]. Journal of Physical and Chemical Reference Data, 1982, 11(Supplement 2): 1−392.

Zn(II)−NH_3−Cl^-−H_2O 体系的优势区图

丁治英，陈启元，尹周澜，刘 葵

中南大学 化学化工学院 有色金属资源化学教育部重点实验室，长沙 410083

摘 要：采用化学平衡模拟软件 GEMS 预测了锌湿法冶金过程中涉及的锌在 Zn(II)−NH_3−H_2O 和 Zn(II)−NH_3−Cl^-−H_2O 体系中的溶解度，并构建了其含锌物种分布图和优势区图。采用平衡实验方法测定了相同条件下锌的溶解度，其结果与预测结果相吻合。含锌物种的分布图和优势区图表明，在弱碱性条件下，2 个体系均为以锌氨和羟基锌氨配合物为溶液的主要物种，其中 $Zn(NH_3)_4^{2+}$ 为主要优势物种；在 Zn(II)−NH_3−Cl^-−H_2O 体系中，锌氨氯三元配合物的形成能有效增大锌在中性条件下的溶解度，在该体系中存在 $Zn(OH)_2$、$Zn(OH)_{1.6}Cl_{0.4}$ 和 $Zn(NH_3)_2Cl_2$ 3 种固相，固相产物的形成取决于体系中总锌、总氨和总氯浓度。这些热力学平衡图表明了体系中各种物种之间的相互影响作用，并预测了总氨和总氯浓度的变化对锌溶解度的影响，为锌湿法冶金提供了热力学数据。

关键词：热力学；优势区图；锌湿法冶金；氨浸

(Edited by Xiang-qun LI)